Polímeros
ISSN 1678-5169 (Online)

https://doi.org/10.1590/0104-1428.20210026

ORIGINAL ARTICLE

Chitosan-based hydrogel for treatment of temporomandibular joint arthritis

Fabianne Lima[1], Wanderson Gabriel Melo[2], Maria de Fátima Braga[2], Ewerton Vieira[3], João Victor Câmara[4]*, Josué Junior Pierote[5], Napoleão Argôlo Neto[6], Edson Silva Filho[3] and Ana Cristina Fialho[1]

[1]Departamento de Patologia e Clínica Odontológica, Universidade Federal do Piauí – UFPI, Terezina, PI, Brasil

[2]Centro de Ciências Agrárias, Universidade Federal do Piauí – UFPI, Terezina, PI, Brasil

[3]Departamento de Química, Centro de Ciências da Natureza, Universidade Federal do Piauí – UFPI, Terezina, PI, Brasil

[4]Departmento de Ciencias Biológicas, Faculdade de Odontologia de Bauru, Universidade de São Paulo – USP, Bauru, SP, Brasil

[5]Departamento de Odontologia, Universidade de Santo Amaro – UNISA, São Paulo, SP, Brasil

[6]Núcleo Integrado de Morfologia e Pesquisas com Células-tronco, Universidade Federal do Piauí – UFPI, Terezina, PI, Brasil

**jvfrazao92@hotmail.com*

Abstract

To produce polysaccharide-based hydrogels and cerium (Ce3+) doped hydroxyapatite plus chitosan and collagen to enable future applications in the treatment of joint degeneration. Hydrogel production and characterization were performed with Fourier transform infrared spectroscopy (FTIR), thermogravimetry analysis (TGA) and cytotoxicity testing with MTT [3-(4,5-dimethylthiazol-2-yl)-2,5-diphenyltetrazolium bromide]. A final biomaterial composition was Kelcogel® Gelana (58%), chitosan (22.3%), Ce3+ doped hydroxyapatite (10.7%) and bovine collagen (9%), or selected aspect material gelatinous physical color with whitish color and can be injected. The biomaterial composition was proven in the FTIR and TGA, which also provided the maximum supported temperature. In the MTT assay, despite the reduction in viability of the experimental group compared to the control group, cell viability remained approximately 90%. In the FTIR and TGA tests, the material composition was proven. The material does not present cytotoxic behavior for the MTT test, being an alternative for the treatment of joint diseases.

Keywords: *hydrogel scaffold, natural polysaccharides, joint arthritis.*

How to cite: Lima, F., Melo, W. G., Braga, M. F., Vieira, E., Câmara, J. V., Pierote, J. J., Argôlo Neto, N., Silva Filho, E., & Fialho, A. C. (2021). Chitosan-based hydrogel for treatment of temporomandibular joint arthritis. *Polímeros: Ciência e Tecnologia*, *31*(2), e2021019. https://doi.org/10.1590/0104-1428.20210026

1. Introduction

Osteoarthritis (OA) is a slow-progressing chronic degenerative joint disease that causes pain and inability to function. It is characterized by degeneration of the articular cartilage and changes in the structure of the cartilage and the underlying subchondral bone. More recent studies have shown that OA affects not only the articular cartilage, but the entire joint, synovial fluid, calcified cartilage and subchondral bone[1]. The treatment of OA is related, basically, to the use of anti-inflammatory drugs, opioids, analgesics, hormonal drugs and Chinese medicine methods[2]. The use of these treatment routes brings with it a wide variety of side effects and, to date, no drug treatment has been able to provide progressive reversibility of the disease[3]. Therefore, patients resort to non-surgical treatments such as arthrocentesis and, in patients refractory to non-surgical treatment, arthroplasty is an alternative that has traditionally been shown to be more efficient. However, surgical techniques often lead to additional complications and new repair surgeries are often necessary[4,5].

Polysaccharides and biopolymers have been important tools for prevention and in situ treatment of bone and cartilage areas affected by OA. Its clinical application is associated with characteristics of biodegradability, biocompatibility, biofunctionality and non-toxicity[2,4]. This biomaterial has the capacity to establish chemical bonds with living bone and cartilage tissue due to its structure and chemical composition, which are similar to the apatite found in the human skeleton[6].

Gellan gum is an anionic bacterial polysaccharide derived from the bacterium Pseudomonas elodea. Its molecular composition has a tetrasaccharide repeat unit, which consists

of two molecules of D-glucose, one of L-rhamnose and one of D-glucuronic acid. The gelano is, structurally, a double helix, formed by two triple helical chains, left-handed and interlaced. This helical geometry is promoted by the connection in the gelano repeating unit. It is well known that gellan gum can form hydrogels, which consist of a three-dimensional polymeric network that retains large amounts of water and are promising biomaterials in the treatment of joint degenerations[7,8].

The use of biopolymers such as chitosan and collagen for the preparation of hydrogels has proved to be a good alternative. Collagen is the most abundant protein in mammalian tissues and can modify cell morphology and differentiation, enabling significant biocompatibility when applied in tissue engineering. However, it has insufficiency as an injectable property[9-11]. Chitosan, a natural polysaccharide, is a biocompatible polymer that exhibits a wide variety of useful biological properties, such as anti-cholesterol actions and ion sequestration. Due to their molecular structure and a large active surface area, cellulose fibers can be an ideal matrix for the design of bioactive, biocompatible and intelligent materials[12].

Hydroxyapatite (HAp) ensures greater graft stability, as it promotes improved integration of the cartilage projected into the bone matrix by creating an intermediate transition zone rich in calcium phosphate[13]. The addition of Ce3+ salts has been used as an adjunct in the formulation of hydroxyapatite composites due to its good osteoconductive capacity and efficient antimicrobial activity, which allows a significant improvement in the regeneration of bone tissue and a slight improvement in its mechanical properties[14].

This biomaterial is still relatively unknown in the biomedical community and few studies have explored it for tissue engineering. Like alginate, gellan gum can be used for encapsulation and in vitro culture of cells[15,16]. Gellan gum hydrogels were able to develop nasal chondrocytes and, when injected, were efficient in encapsulating and supporting human articulation chondrocytes, in addition to allowing active synthesis of extracellular matrix components[17]. Also, Kelcogel® Gel Gum is a polysaccharide produced by fermentation and used as a gelling agent that forms gels in contact with mono-, di- and multivalent ions. It was used in this work because it has excellent suspension, low impact on viscosity and stabilization. The present study aimed to produce and characterize a hydrogel based on Kelcogel® gellan gum, hydroxyapatite doped with Ce^{3+}, chitosan and bovine collagen, for application in the treatment of joint degenerations in the temporomandibular joint.

2. Materials and Methods

2.1 Hydrogel production

The hydrogel was produced at the Interdisciplinary Laboratory of Advanced Materials at the Federal University of Piauí (LIMAV/UFPI). The synthesis of the hydrogel occurred in four stages: 1. Weighing all the components of the hydrogel; 2. Dissolution of chitosan in 0.25% v/v lactic acid solution; 3. Addition of Ce3+ doped hydroxyapatite to form a suspension; 4. Addition of collagen; 5. Addition of gelanine. In all stages, the system was kept under magnetic stirring, for about 30 minutes until the complete dissolution of each component (Agitator Fisatom Mod.752A/3). After shaking, Gelana hydrogel, chitosan, hydroxyapatite and collagen were stored in a cooled environment. After the process, the pH of the hydrogel was analyzed with the aid of a pH-meter.

2.2 Hydrogel characterization

2.2.1 Fourier transform infrared spectroscopy

To confirm the production of the hydrogel, Fourier transform infrared spectra (FTIR) of the biomaterial and its components were obtained in a spectrophotometer with attenuated total reflectance (ATR). Transmittance mode and wavelength between 400 and 4000 cm^{-1} were used.

2.2.2 Thermal analysis

The technique of thermogravimetric analysis (TGA) was used to evaluate the stability and thermal decomposition of the polymer obtained as a function of the loss of mass. The thermal analyzer was standardized with a heating rate of 10°C/min, in a nitrogen atmosphere, up to a temperature of 600°C and a sample mass of approximately 7 mg.

2.2.3 Cytotoxicity analysis - MTT assay

The MTT [3-(4,5-dimethylthiazol-2-yl)-2,5-diphenyltetrazolium bromide] assay was performed to assess the cytotoxicity of the hydrogel using mesenchymal stem cells from adipose tissue of wistar rats (CTMTA) . A sample of the hydrogel was diluted in α-MEM medium in order to obtain a homogeneous mixture. Then, 100 μL of α-MEM medium and 10^4 CTMTA were added per well in a 96-well plate and incubated for 24 hours for cell adhesion. After two washes with culture medium to remove cells that did not adhere, the hydrogel solution was tested in triplicate, added with α-MEM in each well, with a final volume of 100 μL and incubated for 24, 48 and 72h. Cells in wells without any addition of hydrogel served as a negative control considered 100% viability. Following the incubation period, 10 μL of MTT diluted in α-MEM at 5 mg/mL were added to each well and the plate was incubated again for 5h. The supernatant was discarded and 100 μL of DMSO was added to dissolve the formed formazan crystals, and these were measured at an optical density of 550 nm in a plate reader. The results were compared and analyzed statistically using the Student's t test.

3. Results and Discussions

3.1 Obtaining hydrogels

The final composition of the biomaterial was Gelana Kelcogel® (58%), chitosan (22.3%), Ce3+ doped hydroxyapatite (10.7%) and bovine collagen (9%) and revealed a gelatinous physical appearance with a whitish color and possible to be injected. The pH obtained at the end of the process was 4.7 at a temperature of 29.5°C.

3.2 Fourier transform infrared spectroscopy

In Figure 1, it is possible to observe the similarity of the chitosan spectrum with the spectrum presented in

the hydrogel. In both, it is possible to visualize an axial stretching band of OH, attributed to the hydroxyl group present in chitosan between 3440 to 3480 cm^{-1}; the bands in the 2854 cm^{-1} region are assigned to the CH_2 groups of the pyroses. All characteristic bands are very similar to those reported in the literature[18-20].

For hydroxyapatite, at 3571 cm^{-1}, we can see in Figure 1 the symmetrical stretching mode, due to the hydroxyapatite OH- groups. The region, which ranges from 3700 to 2500 cm^{-1}, has wide bands due to the stretching of hydrogen bound to water molecules (H_2O). The band around 1638 cm^{-1} is derived from the deformation mode of water molecules (H_2O). The 700 to 500 cm^{-1} region presents bands at 632 cm^{-1}, referring to the oscillation mode of ions - OH and the bands at 602, 563 and 575 cm^{-1} are due to the antisymmetric deformation modes of phosphates[21].

From the peaks obtained through the characterization of the gellan gum by FTIR (Figure 2), the assignment of a transmittance band at 3411 cm^{-1} for the gellan gum, which indicates the stretching vibration of the OH^- group in the gelan hydrogel, was demonstrated. The peak at 1051.11 cm^{-1} in gellan gum is attributed to the stretching vibration of C-O[22].

3.3 Thermal analysis

The thermogravimetry (TG) and derived thermogravimetry (DTG) curves in Figure 3 reveal a peak between 86°C and 96°C characterizing the loss of mass. This loss is related to the vaporization of H_2O contained in the polymer and the volatile compounds produced. This loss percentage allows to estimate the amount of water present in the samples, about 90%. This result is in agreement with the results of the OH ligament presented in the FTIR[23].

3.4 Toxicity test - MTT test

The MTT assay assesses cellular metabolic activity and, despite the reduction in absorbance, statistically significant only in the first 24 hours, of the experimental group in relation to the control group, the percentage of cell viability increased when it remained in contact with the hydrogel in 48 and 72 hours (Figure 4). Within 72 hours, cell viability approached the control group with 94.7% viable cells. Thus, the hydrogel did not show cytotoxic behavior for the tested concentration, being compatible with previous studies[24,25].

Due to the reaction between the components and the greater composition of water, the infrared spectrum of the hydrogel assumes characteristics of the spectra of its composition. When observing the spectra of the chitosan sample in Figure 1, overlapping bands of the amides and OH groups of the pyranoses are observed in the regions between 1661 to 1671 cm^{-1}; angular deformation of N-H (between 1583 to 1594 cm^{-1}), the mode referring to the amides is observed in the region of 1500 cm^{-1} and between 1200-800 cm^{-1} the vibrations are associated with the chemical bonds of pyraneses. The bands in the 1640 cm^{-1} region are attributed to the axial deformation C = O of the carbonyl called νC =O, of the acetamide group, which corresponds to the acetylated part of chitosan. The bands in the 1500 cm^{-1} range correspond to the N-H vibration in the plane called νN-H. The bands around 1300 and 1400 cm^{-1} correspond to the symmetrical angular deformation of the CH_3 group[18-20].

For hydroxyapatite, at 3571 cm^{-1}, we can see in Figure 1, the symmetrical stretching mode, due to the hydroxyapatite OH- groups. The weak intensity bands in the region between 2200 to 1950 cm^{-1} are due to the combinations and overlapping of the phosphate stretching modes (PO4).

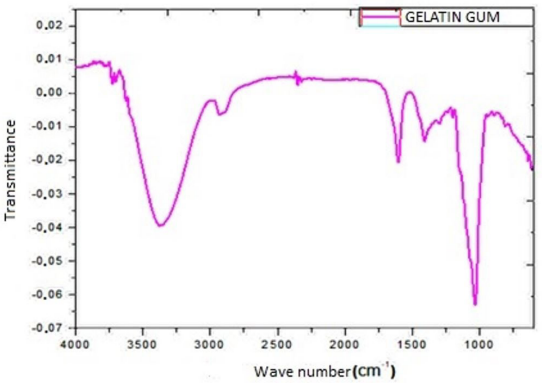

Figure 2. FTIR spectra for gellan gum.

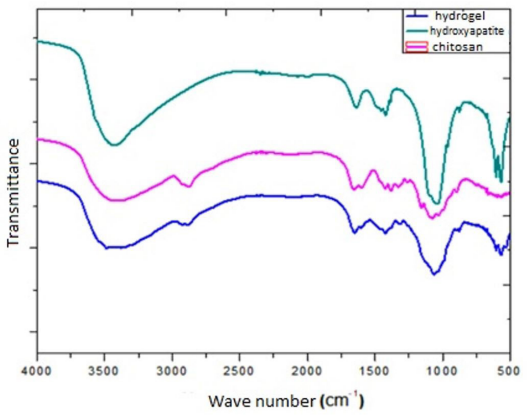

Figure 1. FTIR spectra for the hydrogel components.

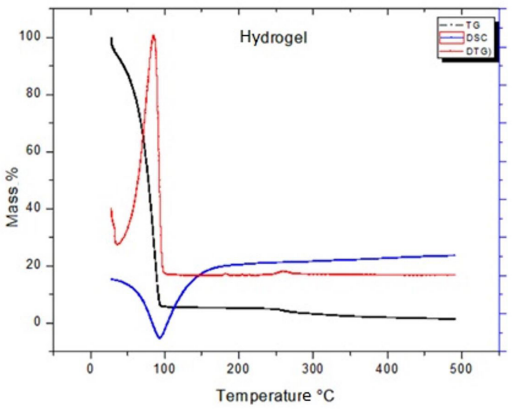

Figure 3. Hydrogel TG, DTG and Differential Exploratory Calorimetry (DSC) curves.

Figure 4. Comparative graph of cell viability.

The intense bands that appear at 1093 cm^{-1} and the doublet around 1040 cm^{-1} originate from the anti-symmetric stretching of the phosphates and the band at 962 cm^{-1} is due to the symmetrical stretching of the phosphates. The 700 to 500 cm^{-1} region presents bands at 632 cm^{-1}, referring to the oscillation mode of the OH^- ions, and the bands at 602, 563 and 575 cm^{-1} are due to the antisymmetric deformation modes of the phosphates[21].

Hydrophilia, which has been reported to be the main factor for the hydrogel water molecules' trapping ability, is contributed by the presence of hydroxyl, carboxyl, sulfonic, amidic and primary amidic functional groups. From the peaks obtained through the characterization of the gellan gum by FTIR, the assignment of a transmittance band at 3411 cm^{-1} for the gellan gum, which indicates the stretching vibration of the OH^- group in the gelan hydrogel, was demonstrated. The peak at 1051.11 cm^{-1} in gellan gum is attributed to the stretching vibration of C-O[22].

DTG results from the TG curve as a function of time or temperature. The recorded peaks represent each mass loss event [9]. The TG / DTG curves of the hydrogels showed a first event between 25°C to 96°C related to the dehydration process. Hydrogel formulated with ASF interpenetrating polymer A B C (Sercin-NIPAAm-AgNPs) showed peaks of decomposition at 303.7°C and 351.2°C associated with the degradation process[25]. In another study, the TG curve in chitosan-based hydrogels showed initial weight loss at 100°C, associated with the dehydration process also present in this study[22].

The samples presented a second mass loss event at 250°C, indicating the beginning of polymer degradation[26]. The DSC curve reveals endothermic and exothermic stages of the samples. The endothermic curves were observed between the ranges of 21°C and 45°C in the hydrogel, the peaks varied between 25 and 35°C. These events help to understand the formation of the hydrogel since they can be associated with the process of the sol-gel transition of the sample.

Due to their hydrophilic characteristic, GG hydrogels provide an ideal environment with the necessary hydration for recovery from injuries, not allowing cytotoxic reactions to the body[27]. The result of this work reveals that the mass of the hydrogels is formed, in large part, by H_2O, linked to the gellan gum through the junction zones previously mentioned, revealing an extremely important characteristic for this application[8]. The loss of mass at a temperature of 90°C makes the sterilization process with humid heat unfeasible, carried out in an autoclave at 121°C. The impossibility of sterilization with moist heat due to the damage to the material's physical characteristics, suggests the need for further studies to evaluate the use of other methods in order to make its clinical application in the treatment of OA viable[23].

To evaluate the cytotoxicity of cells, the MTT assay was performed, which allowed the quantification of cell viability and proliferation in hydrogels[9]. Test samples that reduce cell viability to values below 70% should be considered cytotoxic[28]. It was necessary to use cells with easy access, which allow in vitro expansion and the potential for differentiation into chondrocytes. The cell types used in this study, stem cells from adipose tissue, meet these criteria[29].

In the initial 24 hours, the decrease in cell viability may occur due to the adaptation of cells in the presence of the material, this initial reduction is also observed in another study with hydrogels[30]. Within 72 hours, the cell viability of the gel group approached the control group, with approximately 95% viable cells. Thus, the hydrogel did not show cytotoxic behavior at the concentrations tested, being compatible with previous studies[31-33].

4. Conclusions

During the characterization of the hydrogel, through Fourier transform infrared spectroscopy (FTIR) it was possible to confirm its production. In the thermogravimetric analysis (TGA), the maximum temperature supported by the biomaterial was found to be between 86°C and 96°C. The cytotoxicity analysis by the MTT assay showed low toxicity to cells, allowing cell viability above 90% in 72 hours, positive result for the application of the biomaterial. The production of hydrogels based on polysaccharides and hydroxyapatite doped with Ce3+ plus chitosan and collagen has shown satisfactory results so far and will enable a new low-cost treatment alternative for joint diseases.

5. References

1. Turnbull, G., Clarke, J., Picard, F., Riches, P., Jia, L., Han, F., Li, B., & Shu, W. (2017). 3D bioactive composite scaffolds for bone tissue engineering. *Bioactive Materials*, *3*(3), 278-314. http://dx.doi.org/10.1016/j.bioactmat.2017.10.001. PMid:29744467.

2. Chen, Q., Shao, X., Ling, P., Liu, F., Han, G., & Wang, F. (2017). Recent advances in polysaccharides for osteoarthritis therapy. *European Journal of Medicinal Chemistry*, *139*, 926-935. http://dx.doi.org/10.1016/j.ejmech.2017.08.048. PMid:28881287.
3. Onuora, S. (2017). Osteoarthritis: UCMA links cartilage and bone in OA. *Nature Reviews. Rheumatology*, *13*(3), 130. http://dx.doi.org/10.1038/nrrheum.2017.9. PMid:28202914.
4. Zhang, D., Hu, Z., Zhang, L., Lu, S., Liang, F., & Li, S. (2020). Chitosan-based thermo-sensitive hydrogel loading oyster peptides for hemostasis application. *Materials*, *13*(21), 5038. http://dx.doi.org/10.3390/ma13215038. PMid:33182319.
5. Vincent, T. L., & Watt, F. E. (2018). Osteoarthritis. *Medicine*, *46*(3), 187-195. http://dx.doi.org/10.1016/j.mpmed.2017.12.009.
6. Qindeel, M., Khan, D., Ahmed, N., & Khan, S. (2020). Surfactant-free, self-assembled nanomicelles-based transdermal hydrogel for safe and targeted delivery of methotrexate against rheumatoid arthritis. *ACS Nano*, *14*(4), 4662-4681. http://dx.doi.org/10.1021/acsnano.0c00364. PMid:32207921.
7. Scognamiglio, F., Travan, A., Donati, I., Borgogna, M., & Marsich, E. (2020). A hydrogel system based on a lactose-modified chitosan for viscosupplementation in osteoarthritis. *Carbohydrate Polymers*, *248*, 116787. http://dx.doi.org/10.1016/j.carbpol.2020.116787. PMid:32919575.
8. Zoratto, N., & Matricardi, P. (2018). Semi-IPN- and IPN-Based Hydrogels. *Advances in Experimental Medicine and Biology*, *1059*, 155-188. http://dx.doi.org/10.1007/978-3-319-76735-2_7. PMid:29736573.
9. He, Z., Wang, B., Hu, C., & Zhao, J. (2017). An overview of hydrogel-based intra-articular drug delivery for the treatment of osteoarthritis. *Colloids and Surfaces B, Biointerfaces*, *154*, 33-39. http://dx.doi.org/10.1016/j.colsurfb.2017.03.003. PMid:28288340.
10. Saeedi, T., Alotaibi, H. F., & Prokopovich, P. (2020). Polymer colloids as drug delivery systems for the treatment of arthritis. *Advances in Colloid and Interface Science*, *285*, 102273. http://dx.doi.org/10.1016/j.cis.2020.102273. PMid:33002783.
11. Chuah, Y. J., Peck, Y., Lau, J. E., Hee, H. T., & Wang, D. A. (2017). Hydrogel based cartilaginous tissue regeneration: recent insights and technologies. *Biomaterials Science*, *5*(4), 613-631. http://dx.doi.org/10.1039/C6BM00863A. PMid:28233881.
12. Benltoufa, S., Miled, W., Trad, M., Slama, R. B., & Fayala, F. (2020). Chitosan hydrogel-coated cellulosic fabric for medical end-use: antibacterial properties, basic mechanical and comfort properties. *Carbohydrate Polymers*, *227*, 115352. http://dx.doi.org/10.1016/j.carbpol.2019.115352. PMid:31590862.
13. Dua, R., Comella, K., Butler, R., Castellanos, G., Brazille, B., Claude, A., Agarwal, A., Liao, J., & Ramaswamy, S. (2016). Integration of stem cell to chondrocyte-derived cartilage matrix in healthy and osteoarthritic states in the presence of hydroxyapatite nanoparticles. *PLoS One*, *11*(2), 0149121. http://dx.doi.org/10.1371/journal.pone.0149121. PMid:26871903.
14. Tanaka, T., Matsushita, T., Nishida, K., Takayama, K., Nagai, K., Araki, D., Matsumoto, T., Tabata, Y., & Kuroda, R. (2019). Attenuation of osteoarthritis progression in mice following intra-articular administration of simvastatin-conjugated gelatin hydrogel. *Journal of Tissue Engineering and Regenerative Medicine*, *13*(3), 423-432. http://dx.doi.org/10.1002/term.2804. PMid:30644168.
15. Bordbar, S., Lotfi Bakhshaiesh, N., Khanmohammadi, M., Sayahpour, F. A., Alini, M., & Baghaban Eslaminejad, M. (2020). Production and evaluation of decellularized extracellular matrix hydrogel for cartilage regeneration derived from knee cartilage. *Journal of Biomedical Materials Research. Part A*, *108*(4), 938-946. http://dx.doi.org/10.1002/jbm.a.36871. PMid:31894891.
16. Hemmati-Sadeghi, S., Dey, P., Ringe, J., Haag, R., Sittinger, M., & Dehne, T. (2019). Biomimetic sulfated polyethylene glycol hydrogel inhibits proteoglycan loss and tumor necrosis factor-α-induced expression pattern in an osteoarthritis in vitro model. *Journal of Biomedical Materials Research. Part B, Applied Biomaterials*, *107*(3), 490-500. http://dx.doi.org/10.1002/jbm.b.34139. PMid:29663644.
17. Lee, C., O'Connell, C. D., Onofrillo, C., Choong, P. F. M., Di Bella, C., & Duchi, S. (2020). Human articular cartilage repair: sources and detection of cytotoxicity and genotoxicity in photo-crosslinkable hydrogel bioscaffolds. *Stem Cells Translational Medicine*, *9*(3), 302-315. http://dx.doi.org/10.1002/sctm.19-0192. PMid:31769213.
18. Brugnerotto, J., Lizardi, J., Goycoolea, F. M., Argüelles-Monal, W., Desbrières, J., & Rinaudo, M. (2001). An infrared investigation in relation with chitin and chitosan characterization. *Polymer*, *42*(8), 3569-3580. http://dx.doi.org/10.1016/S0032-3861(00)00713-8.
19. López, F. A., Mercê, A. L. R., Alguacil, F. J., & López-Delgado, A. A. (2008). A kinetic study on the thermal behaviour of chitosan. *Journal of Thermal Analysis and Calorimetry*, *91*(2), 633-639. http://dx.doi.org/10.1007/s10973-007-8321-3.
20. Fráguas, R. M., Simão, A. A., Faria, P. V., Queiroz, E. R., Oliveira, E. N., Jr., & Abreu, C. M. P. (2015). Preparation and characterization chitosan edible films. *Polímeros: Ciência e Tecnologia*, *25*(spe), 48-53. https://doi.org/10.1590/0104-1428.1656.
21. Dourado, E. R. (2006). *Preparação e caracterização de hidroxiapatita nanoestruturada dopada com estrôncio* (Master's thesis). Centro Brasileiro de Pesquisas Físicas, Rio de Janeiro.
22. Ray, R., Maity, S., Mandal, S., Chatterjee, T., & Sa, B. (2010). Development and evaluation of a new interpenetrating network bead of sodium carboxymethyl xanthan and sodium alginate. *Pharmacology & Pharmacy*, *1*(1), 9-17. http://dx.doi.org/10.4236/pp.2010.11002.
23. Causa, F., Netti, P. A., & Ambrosio, L. A. (2007). A multi-functional scaffold for tissue regeneration: the need to engineer a tissue analogue. *Biomaterials*, *28*(34), 5093-5099. http://dx.doi.org/10.1016/j.biomaterials.2007.07.030. PMid:17675151.
24. Majumdar, T., Cooke, M. E., Lawless, B. M., Bellier, F., Hughes, E. A. B., Grover, L. M., Jones, S. W., & Cox, S. C. (2018). Formulation and viscoelasticity of mineralised hydrogels for use in bone-cartilage interfacial reconstruction. *Journal of the Mechanical Behavior of Biomedical Materials*, *80*, 33-41. http://dx.doi.org/10.1016/j.jmbbm.2018.01.016. PMid:29414473.
25. Koh, R. H., Jin, Y., Kim, J., & Hwang, N. S. (2020). Inflammation-modulating hydrogels for osteoarthritis cartilage tissue engineering. *Cells*, *9*(2), 419. http://dx.doi.org/10.3390/cells9020419. PMid:32059502.
26. Kim, H., Mondal, S., Bharathiraja, S., Manivasagan, P., Moorthy, M. S., & Oh, J. (2018). Optimized Zn-doped hydroxyapatite/doxorubicin bioceramics system for efficient drug delivery and tissue engineering application. *Ceramics International*, *44*(6), 6062-6071. http://dx.doi.org/10.1016/j.ceramint.2017.12.235.
27. Cui, Y., Xing, Z., Yan, J., Lu, Y., Xiong, X., & Zheng, L. (2018). Thermosensitive behavior and super-antibacterial properties of cotton fabrics modified with a sercin-NIPAAm-AgNPs interpenetrating polymer Network Hydrogel. *Polymers*, *10*(8), 818. http://dx.doi.org/10.3390/polym10080818. PMid:30960743.
28. Pandey, A., Midha, S., Sharma, R. K., Maurya, R., Nigam, V. K., Ghosh, S., & Balani, K. (2018). Antioxidant and antibacterial hydroxyapatite-based biocomposite for orthopedic applications. *Materials Science and Engineering C*, *88*, 13-24. http://dx.doi.org/10.1016/j.msec.2018.02.014. PMid:29636127.
29. Leone, G., Consumi, M., Pepi, S., Pardini, A., Bonechi, C., Tamasi, G., Donati, A., Lamponi, S., Rossi, C., & Magnani, A.

(2020). Enriched Gellan Gum hydrogel as visco-supplement. *Carbohydrate Polymers*, *227*, 115347. http://dx.doi.org/10.1016/j.carbpol.2019.115347. PMid:31590845.

30. Meschini, S., Pellegrini, E., Maestri, C. A., Condello, M., Bettotti, P., Condello, G., & Scarpa, M. (2020). In vitro toxicity assessment of hydrogel patches obtained by cation-induced cross-linking of rod-like cellulose nanocrystals. *Journal of Biomedical Materials Research. Part B, Applied Biomaterials*, *108*(3), 687-697. http://dx.doi.org/10.1002/jbm.b.34423. PMid:31134760.
31. Wang, B., Zhang, S., Wang, Y., Si, B., Cheng, D., Liu, L., & Lu, Y. (2019). Regenerated Antheraea pernyi Silk Fibroin/Poly(N-isopropylacrylamide) Thermosensitive Composite Hydrogel with Improved Mechanical Strength. *Polymers*, *11*(2), 302. http://dx.doi.org/10.3390/polym11020302. PMid:30960286.
32. Balasubramanian, R., Kim, S. S., & Lee, J. (2018). Novel synergistic transparent k-Carrageenan/Xanthan gum/Gellan gum hydrogel film: mechanical, thermal and water barrier properties. *International Journal of Biological Macromolecules*, *118*(Pt A), 561-568. http://dx.doi.org/10.1016/j.ijbiomac.2018.06.110. PMid:29949745.
33. Dhivya, S., Saravanan, S., Sastry, T. P., & Selvamurugan, N. (2015). Nanohydroxyapatite-reinforced chitosan composite hydrogel for bone tissue repair in vitro and in vivo. *Journal of Nanobiotechnology*, *13*(1), 40. http://dx.doi.org/10.1186/s12951-015-0099-z. PMid:26065678.

Received: Mar. 05, 2021
Revised: July 04, 2021
Accepted: July 18, 2021